25th ABCM International Congress of Mechanical Engineering
October 20-25, 2019, Uberlândia, MG, Brazil

Optimization and passive control for wind turbine with S-airfoil

Wagner Barth Lenz
Federal University of Technology Parana - Campus Ponta Grossa
wagner.barth5@gmail.com
Angelo Marcelo Tusset
Federal University of Technology Parana - Campus Ponta Grossa
Mauricio A. Ribeiro
Federal University of Technology Parana - Campus Ponta Grossa
Jose Manoel Balthazar
Federal University of Technology Parana - Campus Ponta Grossa and Sao Paulo State University (UNESP)

Abstract. *The demand for electric energy has grown in the past two decades. Forcing the conventional method of generation to substitute burning fossil fuel to a more sustainable method, such as wind turbine. Modern wind turbines blade works by lift and is extremely sensitive to the angle of attack. To further improve the efficiency, material and site utilization and other techniques to be optimized. In this paper, it is proposed optimization of design dimensions of the blade by Particle Swarm Optimization. In addition, an uncontrolled and passively controlled wind turbine with spring were compared by numerical simulation using the numerical simulation with the Buhll's methodology of design. The result shows that the spring model improves the performance at lower rotation speeds and prevent overpower the generator at a higher speed.*

Keywords: *Wind Turbine, Passive Control, HAWT*

1. INTRODUCTION

The fuel energy source in the World is shifting to renewable energy. Solar, wind and biomass sources are deemed to replace the main fossil fuel sources. One of the cleanest energy and it has been since 2000 A.C. The wind turbine is divided between VAWT (Vertical Axis Wind Turbine) and HAWT (Horizontal Axis Wind Turbine). The most common for large scale is the HAWT, similar to a windmill. This machines take wind energy and transform it into Rotational energy. The Fig. 1 shows a schematic of a self-regulated HAWT wind turbine.

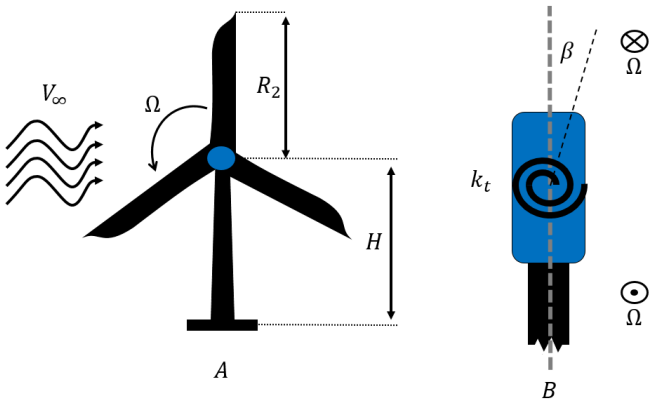

Figure 1. (A) Front view of HAWT, (B) Lateral View, Adapted from: (Wood, 2011; Lenz *et al.*, 2018)

where: V_∞ is the wind speed, R_2 is the external radius, H is the height of the hub, k_t is the torsional spring, Ω is the rotation speed, β is the control angle. The average wind speed is directed influenced by the height of the hub. The speed follows the power law, present on Eq. 1.

$$u = u_r \left(\frac{z}{z_r}\right)^p \tag{1}$$

where: u is the average speed at the desired height, u_r is the speed reference, z_r is the reference height z is the height,

and p is a landscape factor and usually can be used as $\frac{1}{7}$ Holton and Hakim (2012); Hsu *et al.* (1994). The Eq. 1 shows that are more energy at higher than on the ground. However, for long blades, this can cause a very significant increase at the top of rotation to compare to the bottom. This effect is similar to helicopters different speed in blades position Wood (2011). To design the HAWT turbine the Bulh's Methodology was used.

1.1 Bulh's Methodology

Bulh's methodology is an evolution of the Glauert Momentum Theory. This theory is used to calculate the load and torque in each element of a blade and then sum up to create a total, thus having a torque, forces, and power of wind turbine Quandt (1996). Nevertheless, the methodology was a flaw at $a = 0.4$, thus many models were proposed, having similar performance Pratumnopharat and Leung (2011). The wind turbine works by transforming winds kinetic energy of the wind to kinetic energy of rotating the shaft and the generator. The flow over the airfoil combines the rotation with the axial wind speed. This flow is represented in Fig. 2.

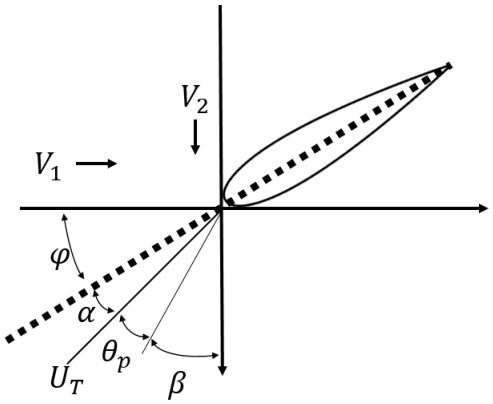

Figure 2. Macro view of a HAWT Adapted from: (Wood, 2011; Lenz *et al.*, 2018)

where: V_1 is the axial speed, V_2 is the radial speed, ϕ is the flow angle, α is the angle of attack, θ_p is the twist angle of the blade, β is the control angle that the spring will change. Thus the sum of angles it is describes the motion on the Eq. 2.

$$\phi = \alpha + \theta_P + \beta \tag{2}$$

Consequently, from Eq.2 it is possible to decompose the force in each element for x and y axis, on Eq. 3.

$$\begin{cases} F_x = F_L cos(\phi) + F_D sin(\phi) \\ F_y = F_L sin(\phi) - F_D cos(\phi) \end{cases} \tag{3}$$

where F_x is the force on the x direction, F_l is the lift force, F_d is the frag force, F_y is the force on the y axis. In addition the speed can be decomposed in each direction as describe on Eq. 4.

$$\begin{cases} U_1 = (1-a)U_0 \\ U_2 = (1+a')r\Omega \\ U_T^2 = U_1^2 + U_2^2 \end{cases} \tag{4}$$

where a is the axial coefficient, a' is the radial coefficient, U_1 is the axial speed, U_2 is the radial speed, r is the local radius, Ω is the rotation speed. The flow angle can be determined by the Eq. 5.

$$\phi = \tan^{-1}\left(\frac{\mathrm{U_1}}{\mathrm{U_2}}\right) \tag{5}$$

Defining the tip speed ration (T_{SR}) in Eq. 6, a parameter of efficiency used to determine the optimization speeds (along the blade), and the Number of Reynolds (R_E) on the following equations. The T_{SR} is an important parameter

because it is directly related to the efficiency and the orientation of the angles. At lower T_{SR} the airfoil does not have the correct orientation of α and high U_T to produce lift. Usually, for commercial turbine it is used between 7 and 10 for HAWT so the airfoil can have enough flow , values higher are not aesthetics pleasing and generate excisive noise Wood (2010).

$$\begin{cases} T_{sr} = \frac{r\Omega}{V_\infty} \\ Re = \nu U_T c \\ \sigma = \frac{Bc}{2\pi r} \end{cases} \tag{6}$$

where, σ is the solidity, B is the number of the blades, c is the chord, r is the local radius, ν is the kinematic viscosity. Because of the discontinuity of the wing, the wing tip generates vortexes and it works as a brake. It will be consider the Prant model to infinitesimal element will be used and it is presented in the Eq. 7:

$$F = \frac{2}{\pi} arcos\left(-e^{\frac{-B(R-r)}{2Rsin\phi}}\right) \tag{7}$$

where, B is the number of blades, R is the length of the blade, r is the local radius. The F is an efficiency parameter due to the wind tip vortex of the blade. The axial and the radial coefficients are defined in Eq. 8:

$$\begin{cases} C_x = C_L cos\phi + C_D sin\phi \\ C_y = C_L sin\phi - C_D cos\phi \end{cases} \tag{8}$$

where, C_x is the axial coefficient, C_y is the radial coefficient, C_L is the lift coefficient, C_D is the coefficient of drag of the airfoil based on the angle of attack and the Reynold Number presented on the Eq.6 and Eq. 5. The a and a', can be calculated as Eq. 9:

$$\begin{cases} a = \frac{\sigma C_x}{4Fsin^2\phi + C_x\sigma} \\ a' = \frac{\sigma C_x}{4Fsin\phi cos\phi - C_y\sigma} \end{cases} \tag{9}$$

if $a > 0.4$, then:

$$\begin{cases} a = \frac{0.5(18\sigma C_x + 36F^2sin^2\phi - 40Fsin^2\phi - 6\sqrt{C_1})}{C_2} \\ C_1 = 18Fsin^2\phi\sigma C_x + 36F^4sin^4\phi - 48F^3sin^4\phi \\ C_2 = 9\sigma C_x - 50Fsin^2\phi + 36F^2sin^2\phi \end{cases} \tag{10}$$

This method is iterative, that means the initial guess as recommend by the author is $a = 0.3$, and $a' = 0.001$. If the a and a' used in Eq. 4 are different from those obtainen in Eq. 9 or 10, this method should be repeated until they converge to an admissible error as recomend of 10^{-3}. A comparison between several model can been seen at Pratumnopharat and Leung (2011). After that, the torque and power on each element can be calculated by the Eq. 11 :

$$\begin{cases} dT_m = 4a'(1-a)\rho_{air}V_\infty\pi r^3\Omega dr \\ P_t = T_m\Omega \end{cases} \tag{11}$$

2. METHODOLOGY

Using the Buhl's methodology, with 15 interactions on so a an a' can converge. The following parameters were used, on Eq. 1, $WindBase = 3.5m/s$, wind corrected by height $V_\infty = 5.37m/s$,$V_{best} = 8.94m/s$,$T_{sr} = 6$. z=1/7. The bounds seleteced are presented on the Table 2.

Table 1. Selected Bound for PSO Otimization

	u_1	u_2	u_3	u_4
Upper Bound	0.05	0.2	0.75	-20
Lower Bound	0.2	0.35	3	20

The airfoil selected were s821,s823,s835,s833,s835,s834. This airfoil has been studied by the NREL (National Renewable Energy Laboratory) because of similar efficiency than the NACA series and reduce noise levels./ Tangler and Somers (1995); Sommers (2005); Griffin (2000); Selig and McGranahan (2004). For the optimization process the Eq. 12 were used to limit the physical characteristics of the blade.

$$\begin{aligned} c(r) &= \frac{u_1}{r} + u_2 \\ \theta_p(r) &= \frac{u_3}{r} + u_4 \end{aligned} \tag{12}$$

where: $c(r)$ is the function of the size of the chord, $\theta_p(r)$ is the function of twist angle of the blade, and the parameters u_n are the parameters to be optimized. Thus, utilizing the parameters on Table 2 for the optimization.

Table 2. PSO Parameter

Swarm Size	406
Function Tolerance	0.00001
Max Stall Iterations	10
Max Iterations	550
Inertia	0.6
Self Adjustment Weight	1
Social Adjustment Weight	1.49
Objective Limit	0.8

These parameters were chosen to accommodate the PSO on Matlab, and to ensure convergence with 10 stall interactions an objective below the maximum possible. The following optimization function was used:

$$\begin{aligned} &\underset{J}{\text{minimize}} \quad J(u_1, u_2, u_3, u_4) = \frac{1}{c_p} \\ &\text{subject to} \\ &0.05 < u_1 < 0.2, .2 < u_2 < .35, T_{sr} = 6, \\ &.75 < u_3 < 3, -20 < u_4 < 20, V_\infty = 5.37 \end{aligned} \tag{13}$$

Using the Eq. 14, with the PSO, the best airfoil will have better c_p. Thus, the k_t of the spring can be calculated, and the dynamic analysis of uncontrolled and a passive wind turbine can be made. Using the V_∞ in two models:

$$V_\infty = \begin{cases} \text{ConstantSpeed}, \ \text{case 1} \\ 5.5 + 5sin(2\pi ft), \ \text{case 2} \end{cases} \tag{14}$$

3. Results

Using the Rayleigh distribution with an average speed of 5.37 [m/s]. The probability distribution and the energy distribution are shown in Fig. 3.

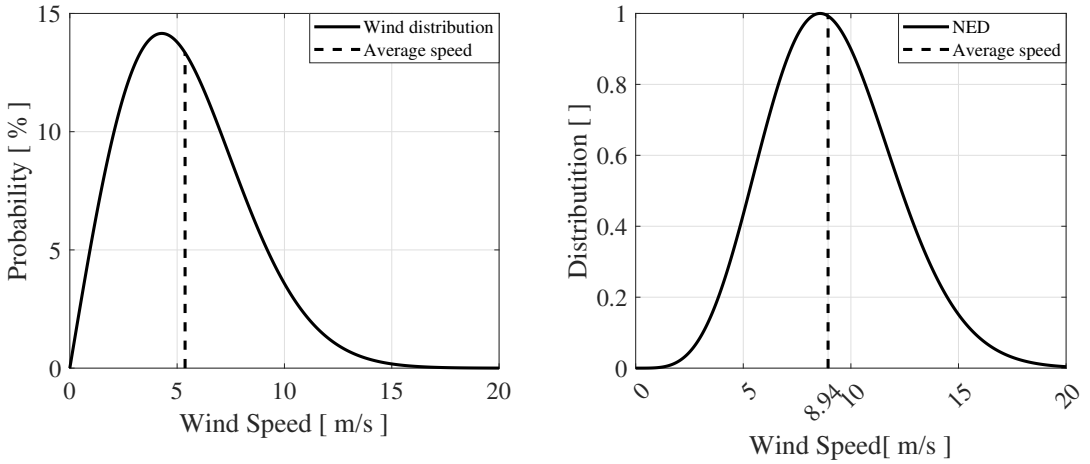

Figure 3. Wind distribution and average wind (A), Normalized wind distribution (NED) and average speed for energy distribution (B)

As shown in Fig. 3, the average wind is $V_\infty = 5.37$. Nevertheless, due to probability and the the power behavior of fluids that increase at third power, the influence of the wind speed and the probability are lagged on the relation with the wind distribution. Consequently, both averages are important. The first average could be used to stabilize the cost/benefit of the site. The second average could be used as a threshold of the production of energy. Thus, the profiles were optimized to average wind speed a the PSO Optimization. The results are presented in Table 3.

Table 3. PSO Otimization Results

u_1	u_2	u_3	u_4	c_p	Airfoil	Interactions
0.1181	0.2008	2.2253	4.1520	0.4257	s834	82
0.1820	0.2008	2.9933	4.2525	0.4178	s835	45
0.1703	0.2002	3.0000	4.8552	0.4171	s833	33
0.1871	0.2003	2.9573	4.6082	0.4128	s835	44
0.1362	0.2032	2.5771	4.4481	0.4098	s823	26
0.1366	0.2000	2.9717	3.8949	0.4022	s821	30

As expected, the PSO optimization results on a similar c_p, because there is minor changes between airfoils. Nevertheless, the best airfoil was S834. This model was selected for the studies of the dynamics, presented below.

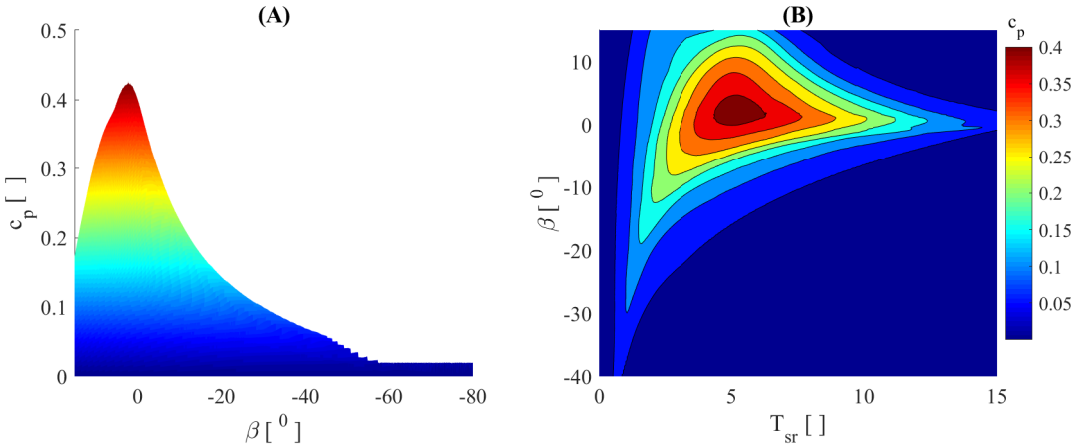

Figure 4. Coefficient of power for selected wind turbine,in A the surface and B is the contour

Thus, the best angle of control and coefficient of power retrieved from the data on Fig. 4.

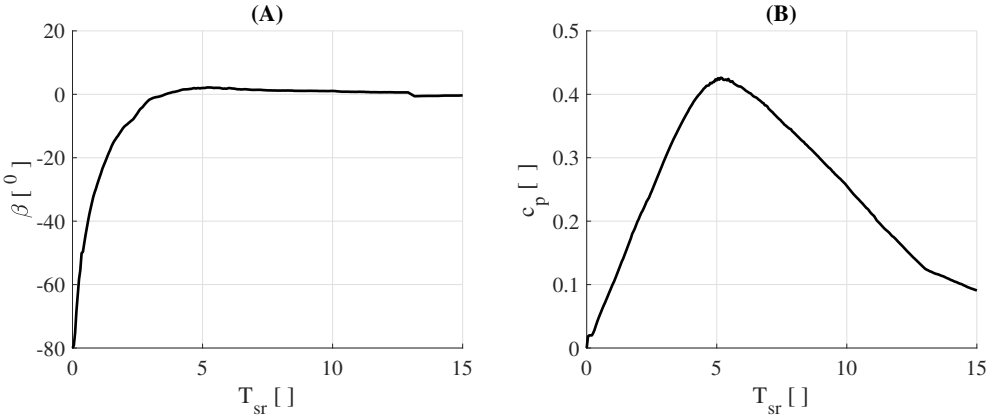

Figure 5. Best from β A, and best c_p on B

Consequently, using the Eq. 6 is possible to obtain the best angle for each rotation at average wind speed. The spring model is using the Minimum squares method to improve the performance at lower rotation and mitigate overpowering the generator. To investigate the effectiveness of the spring, two wind models were used and are presented below:

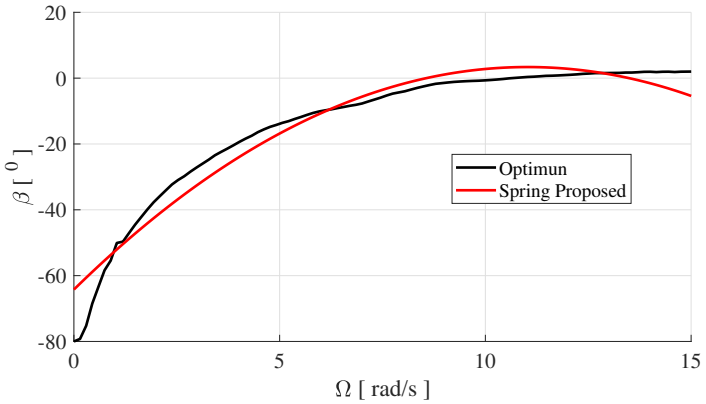

Figure 6. Comparison between the optimum β and the proposed spring behavior

Thus, it was analyzed the dynamic comparing the Ω_{max} $[\mathrm{rad/s}]$ uncontrolled (without spring) and passive controlled (with spring), for 1, 10, 20, and 50 [s] to illustrate the difference of behaviours, for wind case 1 in Fig.7 .

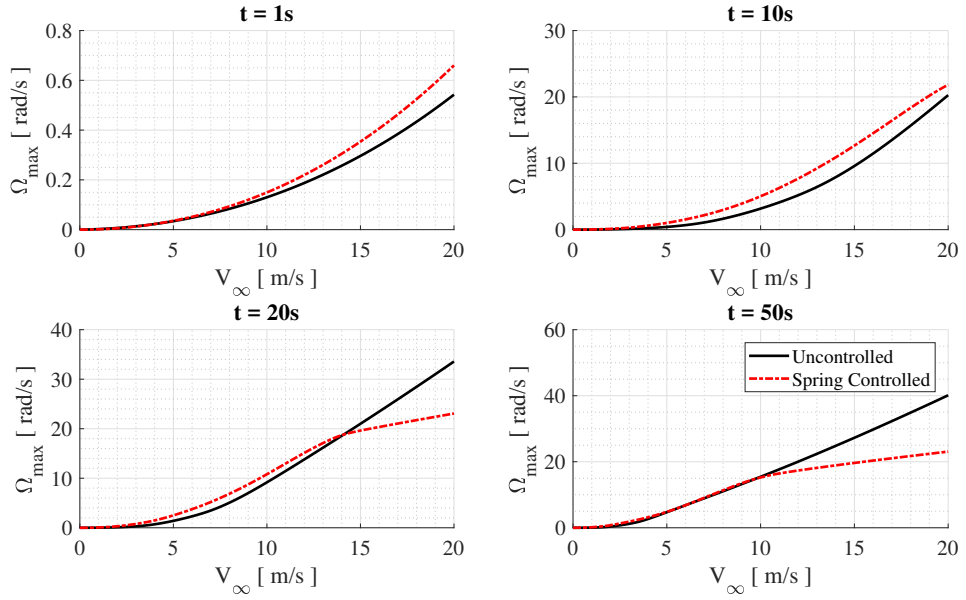

Figure 7. Comparison the Ω_{max} $[rad/s]$ under different frequencies for case 1 (a) Under 1 $[s]$ (b) Under 10 $[s]$,(c) Under 20 $[s]$,(d) Under 50 $[s]$

The same numerical simulation was done for the case, for the same time samples, in Fig. 8.

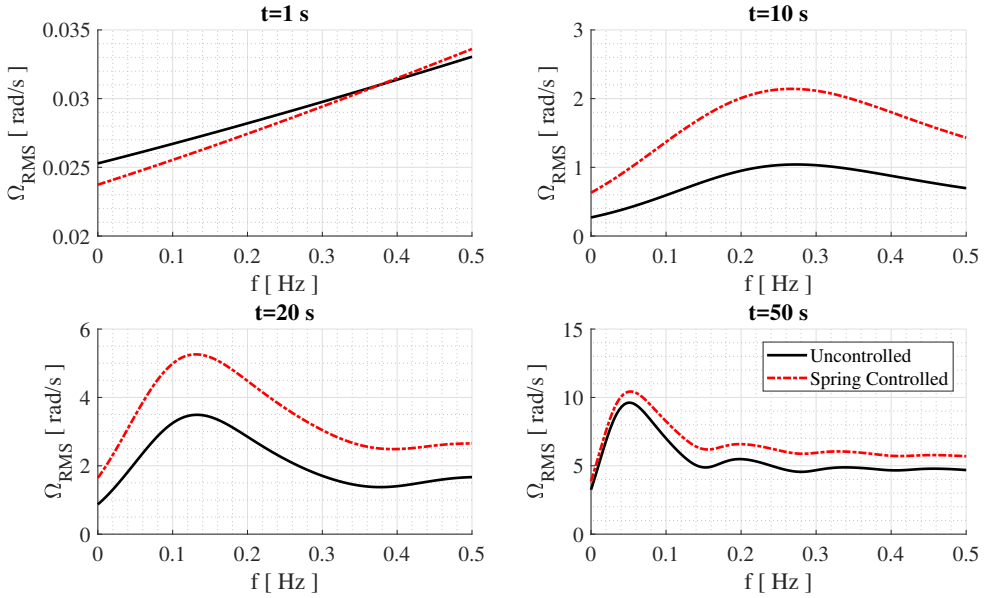

Figure 8. Comparison the Ω_{max} $[rad/s]$ under different frequencies for case 2. (a) Under 1 $[s]$ (b) Under 10 $[s]$,(c) Under 20 $[s]$,(d) Under 50 $[s]$

Expanding the same methodology for the whole spectrum of speed and time. Applying the color scale from the controller wind turbine and the speeds above to be between black to white, it is possible to obtain the Fig. 9.

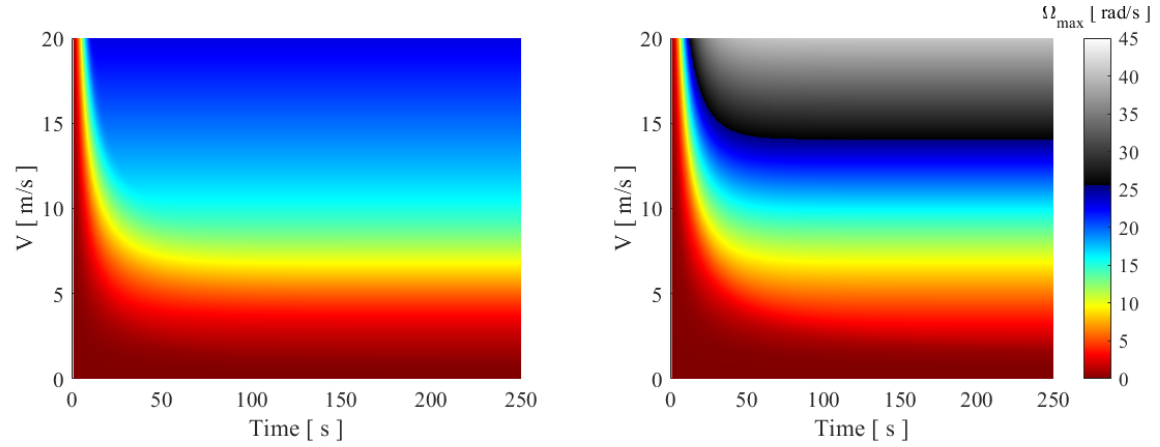

(A) (B)

Figure 9. Comparison of controlled and uncontrolled wind turbine for case 1 (a) Max rotation speed for controlled (b) Max rotation speed for uncontrolled

As shown in Fig. 9, the controller wind turbine restrict the speed during high wind speed in times greater than 25s. Thus, proving efficiency of the spring. Applying the same methodology for case 2 on Fig. 9.

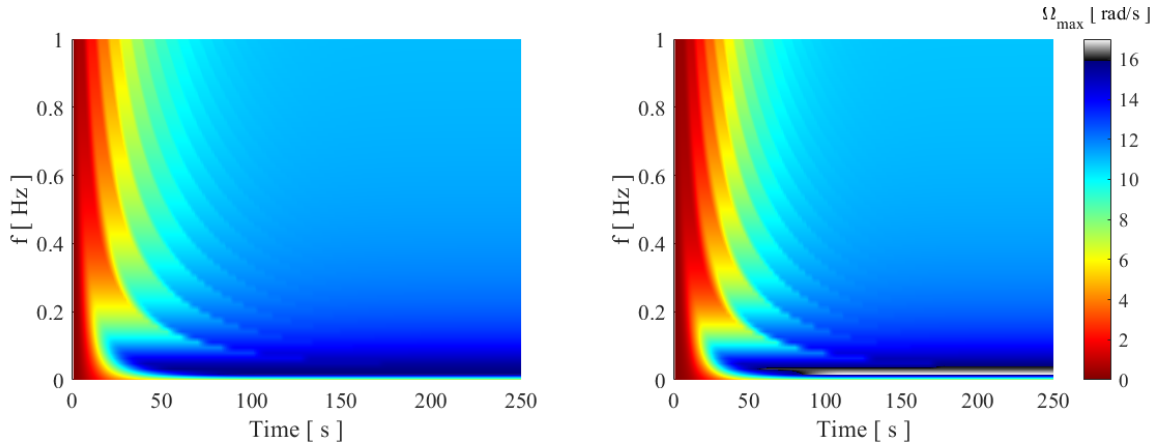

(A) (B)

Figure 10. Comparison of controlled and uncontrolled wind turbine for case 2 (a) Max rotation speed for controlled (b) Max rotation speed for uncontrolled

Comparing the results without and with the controller. It is clear that during high wind speeds oscillations. The spring blocks the excessive rotation, even before then the continuous cases.

4. CONCLUSIONS

The result of the optimization on Table 3 showed that the Airfoil S834 presented better results than the other airfoil. Nevertheless, all the airfoils performed similarly, thus showing that most of the performance was extracted given the bound impose by the chord and torsion angle.

The nonlinear behavior of the optimum angle made necessary a nonlinear spring. Thus, complying with the desire functions: improving the start of the wind turbine as shown in Fig. 7 and Fig. 8. As the wind turbine under 1[s], 10[s] , 20[s] and 50 [s] have a higher rotation speed for case 1 and case 2. In addition at 50[s] on Fig. 7 it mitigates the overpowering of the generator.

Comparing at the whole spectrum at case 1, on Fig. 9 the controlled wind turbine slowing increase the Ω and limiting at 20 [rad/s], whereas the uncontrolled grows until 45[rad/s]. At the case 2, the variation of wind speed did not affect the wind turbine.

5. REFERENCES

Griffin, D.A., 2000. "NREL Advanced Research Turbine (ART) Aerodynamic Design of ART-2B Rotor Blades". Technical report, National Renewable Energy Laboratory. URL `https://www.nrel.gov/docs/fy00osti/28473.pdf`.

Holton, J.R. and Hakim, G.J., 2012. *An Introduction to Dynamic Meteorology, Volume 88 (International Geophysics)*. Academic Press.

Hsu, S.A., Meindl, E.A. and Gilhousen, D.B., 1994. "Determining the power-law wind-profile exponent under near-neutral stability conditions at sea". *Journal of Applied Meteorology*, Vol. 33, No. 6, pp. 757–765.

Lenz, W.B., Tusset, A.M., Rocha, R.T., Janzen, F.C., Kossoski, A. and Balthazar, J.M., 2018. "Genetic algorithm optimization for horizontal axis wind turbine".

Pratumnopharat, P. and Leung, P., 2011. "Validation of various windmill brake state models used by blade element momentum calculation". *Renewable Energy*, Vol. 36, No. 11, pp. 3222–3227.

Quandt, G., 1996. "Wind Turbine Trailing-Edge Aerodynamic Brake Design". Technical report, National Renewable Energy Laboratory.

Selig, M.S. and McGranahan, B.D., 2004. "Wind Tunnel Aerodynamic Tests of Six Airfoils for Use on Small Wind Turbines ". Technical report, National Renewable Energy Laboratory. URL `https://www.nrel.gov/docs/fy00osti/28473.pdf`.

Sommers, D., 2005. "The S819, S820, and S821 Airfoils". Technical report, National Renewable Energy Laboratory. URL `https://www.nrel.gov/docs/fy06osti/39797.pdf`.

Tangler, J. and Somers, D., 1995. "NREL Airfoil Families for HAWTs". Technical report, National Renewable Energy Laboratory. URL `https://www.nrel.gov/docs/fy06osti/39797.pdf`.

Wood, D., 2010. "Small wind turbines for remote power and distributed generation". *Wind Engineering*, Vol. 34, No. 3, pp. 241–254.

Wood, D., 2011. *Small Wind Turbines*. Springer London.